

MULTI-FLORET SPIKELET1, Which Encodes an AP2/ERF Protein, Determines Spikelet Meristem Fate and Sterile Lemma Identity in Rice^{1[C][W]}

Deyong Ren², Yunfeng Li², Fangming Zhao, Xianchun Sang, Junqiong Shi, Nan Wang, Shuang Guo, Yinghua Ling, Changwei Zhang, Zhenglin Yang, and Guanghua He*

Rice Research Institute (D.R., Yu.L., F.Z., X.S., J.S., N.W., S.G., Yi.L., C.Z., Z.Y., G.H.), Chongqing Key Laboratory of Application and Safety Control of Genetically Modified Crops (D.R., Yu.L., F.Z., X.S., J.S., N.W., S.G., C.Z., Z.Y., G.H.), and Engineering Research Center of South Upland Agriculture, Ministry of Education (Yi.L., G.H.), Southwest University, Chongqing 400715, China; and Engineering Research Center of South Upland Agriculture, Ministry of Education, Chongqing 400715, China (Yu.L., F.Z., X.S., N.W., S.G., Yi.L., C.Z., Z.Y., G.H.)

The spikelet is a unique inflorescence structure of grass. The molecular mechanism that controls the development of the spikelet remains unclear. In this study, we identified a rice (*Oryza sativa*) spikelet mutant, *multi-floret spikelet1* (*mfs1*), that showed delayed transformation of spikelet meristems to floral meristems, which resulted in an extra hull-like organ and an elongated rachilla. In addition, the sterile lemma was homeotically converted to the rudimentary glume and the body of the palea was degenerated in *mfs1*. These results suggest that the *MULTI-FLORET SPIKELET1* (*MFS1*) gene plays an important role in the regulation of spikelet meristem determinacy and floral organ identity. *MFS1* belongs to an unknown function clade in the APETALA2/ethylene-responsive factor (AP2/ERF) family. The *MFS1*-green fluorescent protein fusion protein is localized in the nucleus. *MFS1* messenger RNA is expressed in various tissues, especially in the spikelet and floral meristems. Furthermore, our findings suggest that *MFS1* positively regulates the expression of *LONG STERILE LEMMA* and the *INDETERMINATE SPIKELET1* (*IDS1*)-like genes *SUPERNUMERARY BRACT* and *OsIDS1*.

In the reproductive phase of angiosperms, the shoot meristem is transformed into an inflorescence meristem, which then produces a floral meristem from which floral organs begin to develop, according to the mechanism known as the ABCDE model (Coen and Meyerowitz, 1991; Coen and Nugent, 1994; Dreni et al., 2007; Ohmori et al., 2009). An inflorescence can be classified as determinate or indeterminate based on whether its apical meristem is transformed into a terminal floral meristem. In an indeterminate inflorescence, the lateral meristem is permanently differentiated from the apical meristem, which is not

converted into the terminal floral meristem, as occurs during the development of the inflorescences of *Arabidopsis* (*Arabidopsis thaliana*) and snapdragon (*Antirrhinum majus*). In contrast, in a determinate inflorescence, the apical meristem is transformed into the terminal floral meristem after the production of a fixed number of lateral meristems, as occurs during the development of the inflorescences of tobacco (*Nicotiana tabacum*) and tomato (*Solanum lycopersicum*; Bradley et al., 1997; Ratcliffe et al., 1999; Sussex and Kerk, 2001; Chuck et al., 2008).

In general, inflorescences in grasses consist of branches and spikelets (Coen and Nugent, 1994; Itoh et al., 2005; Kobayashi et al., 2010). In these organisms, the branch meristem is determinate. It produces several lateral spikelet meristems, followed by the final production of a terminal spikelet meristem. The spikelet, the specific unit of the grass inflorescence, comprises a pair of bracts and one to 40 florets; it shows determinacy or indeterminacy depending on the species (Clifford, 1987; Malcomber et al., 2006). In species with a determinate spikelet, such as rice (*Oryza sativa*), after the production of fixed lateral floral meristems, the spikelet meristems are converted into terminal floral meristems, resulting in termination of the spikelet meristem fate. In contrast, in species with an indeterminate spikelet, such as wheat (*Triticum aestivum*), the spikelet meristem fate is maintained continuously and produces a variable number of lateral floral meristems.

¹ This work was supported by the National Natural Science Foundation of China (grant no. 31071071), the 863 Program of China (grant no. 2011AA10A100), the "111" Project (grant no. B12006), the Major Research Projects of Chongqing, China (grant no. 2012ggc80002), and the Fundamental Research Funds for the Central Universities, China (grant no. XDJK2010C073).

² These authors contributed equally to the article.

* Corresponding author; e-mail hegh1968@yahoo.com.cn.

The author responsible for distribution of materials integral to the findings presented in this article in accordance with the policy described in the Instructions for Authors (www.plantphysiol.org) is: Guanghua He (hegh1968@yahoo.com.cn).

[C] Some figures in this article are displayed in color online but in black and white in the print edition.

[W] The online version of this article contains Web-only data.

www.plantphysiol.org/cgi/doi/10.1104/pp.113.216044

In Arabidopsis, the gene *TERMINAL FLOWER1* (*TFL1*) was shown to maintain indeterminacy in the fate of the inflorescence. In the *tfl1* mutant, the inflorescence meristems were converted into floral meristems earlier than in the wild type, but the ectopic expression of *TFL1* resulted in the transformation of floral meristems at a later stage of development to secondary inflorescence meristems (Bradley et al., 1997; Ratcliffe et al., 1999; Mimida et al., 2001). In rice, overexpression of either of the *TFL1*-like genes, *RICE CENTRORADIALIS1* (*RCN1*) or *RCN2*, delayed the transition of branch meristems to spikelet meristems and finally resulted in the production of a greater number of branches and spikelets than in the wild type (Nakagawa et al., 2002; Rao et al., 2008).

To date, no gene that acts to maintain the indeterminacy of the spikelet meristem has been reported. However, two classes of genes have been shown to be involved in termination of the indeterminacy of spikelet meristems. One of these is the group of terminal floral meristem identity genes. A grass-specific *LEAFY HULL STERILE1* (*LHS1*) clade in the *SEPALLATA* (*SEP*) subfamily belongs to this class. *LHS1*-like genes were found to be expressed only in the terminal floral meristem in species with spikelet determinacy, which suggested that they exclusively determine the production of the terminal floral meristem, by which the spikelet meristem acquires determinacy (Cacharroón et al., 1999; Malcomber and Kellogg, 2004; Zahn et al., 2005). The other class comprises the *INDETERMINATE SPIKELET1* (*IDS1*)-like genes, which belong to the *APETALA2*/ethylene-responsive factor (*AP2/ERF*) family. Unlike *LHS1*-like genes, this class of genes regulates the correct timing of the transition of the spikelet meristem to the floral meristem but does not specify the identity of the terminal floral meristem. In maize (*Zea mays*), loss of *IDS1* function produces extra florets (Chuck et al., 1998). In addition, mutation of *SISTER OF IDS1* (*SID1*), a paralog of *IDS1* in maize, resulted in no defects in terms of spikelet development. However, the *ids1+sid1* double mutant failed to generate floral organs and instead developed more bract-like structures than are found in wild-type plants (Chuck et al., 2008). The rice genome contains two *IDS1*-like genes, *SUPERNUMERARY BRACT* (*SNB*) and *OsIDS1*. Loss of activity of *SNB* or *OsIDS1* produced extra rudimentary glumes, and *snb+osids1* double mutant plants developed more rudimentary glumes than either of its parental mutants (Lee et al., 2007; Lee and An, 2012). These results revealed that the mutated *IDS1*-like genes prolonged the activity of the spikelet meristem.

In most members of Oryzae, the spikelet is distinct from those of other grasses, in that it comprises a pair of rudimentary glumes, a pair of sterile lemmas (empty glumes), and one floret (Schmidt and Ambrose, 1998; Ambrose et al., 2000; Kellogg, 2009; Hong et al., 2010). The rudimentary glumes are generally regarded as severely reduced bract organs, but the origin of sterile lemmas has been widely debated. Recent studies suggested that the sterile lemmas are the vestigial lemmas

of two lateral florets. The gene *LONG STERILE LEMMA* (*G1*)/*ELONGATED EMPTY GLUME1* (*ELE1*) is a member of a plant-specific gene family. In the *g1/ele1* mutant, sterile lemmas were found to be homeotically transformed into lemmas (Yoshida et al., 2009; Hong et al., 2010). The *OsMADS34* and *EXTRA GLUME1* (*EG1*) genes were also shown to determine the identities of sterile lemmas. In the *osmads34* and *eg1* mutants, the sterile lemmas were enlarged and acquired the identities of lemmas (Li et al., 2009; Gao et al., 2010; Kobayashi et al., 2010). Additionally, the *SEP*-like gene *LHS1/OsMADS1*, which specifies the identities of both the lemma and the palea, was not expressed in sterile lemmas, and ectopic expression in sterile lemmas resulted in the transformation of sterile lemmas to lemmas (Jeon et al., 2000). These findings suggest that the sterile lemma may be homologous to the lemma. Nevertheless, some researchers still considered that the sterile lemmas are instead vestigial bract-like structures similar to the rudimentary glumes (Schmidt and Ambrose, 1998; Kellogg, 2009; Hong et al., 2010).

In this study, we isolated the rice *MULTI-FLORET SPIKELET1* (*MFS1*) gene, which belongs to a clade of unknown function in the *AP2/ERF* gene family. The mutation of *MFS1* was shown to delay the transformation of the spikelet meristem to the floral meristem and to result in degeneration of the sterile lemma and palea. These results suggest that *MFS1* plays an important role in the regulation of spikelet determinacy and organ identity. Our findings also reveal that *MFS1* positively regulates the expression of *G1* and the *IDS1*-like genes *SNB* and *OsIDS1*.

RESULTS

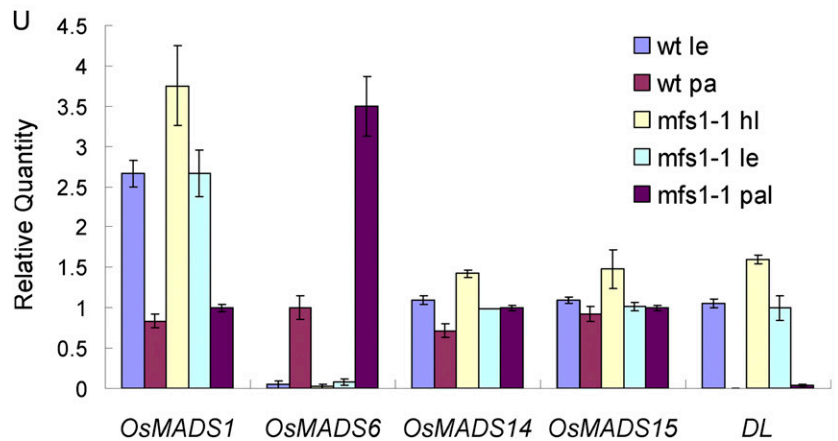
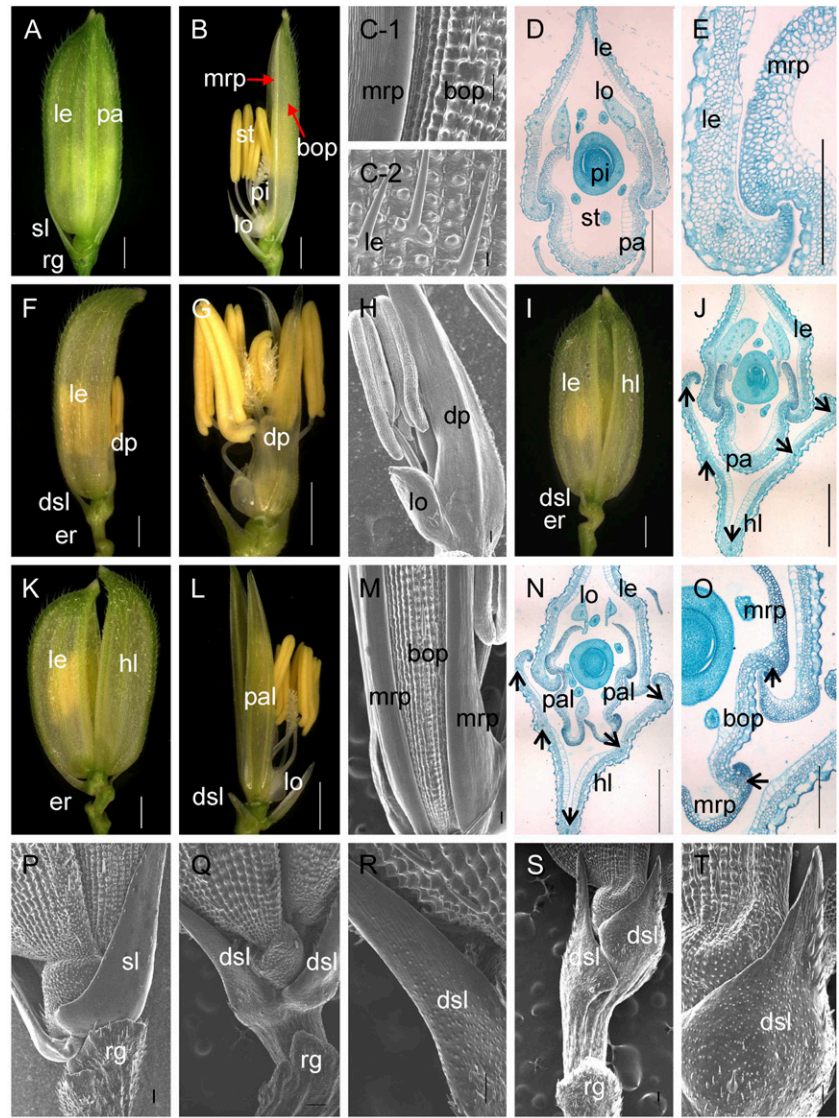
We identified two recessive mutants related to the development of the rice spikelet, *mfs1-1* and *mfs1-2* (Fig. 1; Supplemental Fig. S1). An allelism test revealed that the two mutants were allelic. Given that *mfs1-1* showed more severe defects than *mfs1-2*, the rest of this paper focuses primarily on the *mfs1-1* mutant.

mfs1-1 Shows Pleiotropic Defects in Spikelet Development

Generally, a wild-type rice spikelet consists of one pair of rudimentary glumes, one pair of sterile lemmas, and one terminal fertile floret. The floret comprises four whorls of floral organs: one lemma and one palea in whorl 1, two lodicules in whorl 2, six stamens in whorl 3, and one pistil with two stigmas in whorl 4 (Fig. 1, A and B).

In wild-type spikelets, the sterile lemma was shown to be larger than the rudimentary glume (Fig. 1A). Most of the epidermis of the sterile lemma was smooth and consisted of regularly arranged flat cells and rare cells with trichomes on the abaxial side (Fig. 1P). The epidermal cells of rudimentary glumes were arranged irregularly and bore lots of protrusions and trichomes (Fig. 1P). In contrast, the sterile lemma was found to be

Figure 1. Phenotypes of spikelets in the wild-type and *mfs1-1*. A and B, Wild-type spikelet. C-1, Epidermal surface of wild-type palea. C-2, Epidermal surface of wild-type lemma. D and E, Histological analysis of wild-type spikelet. F and G, *mfs1-1* spikelet with a degenerated palea. H, Epidermal surface of the degenerated palea in G. I, *mfs1-1* spikelet with an extra hull and a normal palea. J, Histological analysis of *mfs1-1* spikelet with an extra hull and a normal palea. K and L, *mfs1-1* spikelet with an extra hull and degenerated paleae. M, Epidermal surface of the degenerated palea in L. N and O, Histological analysis of an *mfs1-1* spikelet with an extra hull and degenerated paleae. P, Epidermal surface of the sterile lemma and rudimentary glume in the wild type. Q to T, Epidermal surface of the degenerated sterile lemma and rudimentary glume in *mfs1-1*. U, Relative expression levels of floral organ identity genes in wild-type (wt) and *mfs1-1* floral organs. dp, Degenerated palea; dsl, degenerated sterile lemma; er, elongated rachilla; hl, hull (lemma/palea)-like organ; le, lemma; lo, lodicule; pa, palea; pal, palea-like organ; pi, pistil; rg, rudimentary glume; sl, sterile lemma; st, stamen. Black arrows represent vascular bundles. Bars = 1,000 μm in A, B, F, G, I, K, and L and 100 μm in C to E, H, J, M, and N to T. Error bars in U indicate sd.



reduced to various degrees, even resembling the rudimentary glume in size in the *mfs1-1* mutant (Fig. 1, F, I, and L; Supplemental Fig. S1). The abundant protrusions and trichomes were borne on the middle and

lower epidermis of degenerated sterile lemmas, which were highly similar to those of the rudimentary glume (Fig. 1, Q–T). Meanwhile, the regular and smooth cells, like those of the sterile lemma of the wild type, still

remained on the top region of the degenerated sterile lemmas (Fig. 1, Q–T). These results indicated that the degenerated sterile lemma in the *mfs1-1* mutant had the identities of both sterile lemmas and rudimentary glumes.

It was found that 65% of *mfs1-1* spikelets developed an extra hull (lemma/palea)-like organ (Fig. 1, I and K; Supplemental Fig. S1A). The wild-type lemma had four cell layers, silicified cells, fibrous sclerenchyma, spongy parenchymatous cells, and nonsilicified cells, and developed five vascular bundles. Compared with the lemma, the palea had three vascular bundles and consisted of two parts: the body of the palea (bop) and two marginal regions of the palea (mrp). The cellular structure of the bop was very similar to that of the lemma, but the mrp displayed a distinctive smooth epidermis, which lacked the epicuticular silicified thickening found in the lemma and bop (Fig. 1, B–E). In the *mfs1-1* mutant, the extra hull-like organ showed a similar histological structure and had five vascular bundles, resembling the wild-type lemma (Fig. 1, J and N). We detected the mRNA levels of the lemma identity gene *DROOPING LEAF (DL)*, the lemma and palea identity genes *OsMADS1*, *OsMADS14*, and *OsMADS15*, and the mrp identity gene *OsMADS6* in *mfs1-1* extra hull-like organs. Abundant levels of *OsMADS1*, *OsMADS14*, *OsMADS15*, and *DL* transcripts were detected, but no *OsMADS6* expression was found (Fig. 1U). These results revealed that the extra hull-like organ had the identity of the lemma.

In *mfs1-1* spikelets with extra lemma-like organs, 38% had no normal palea. Two palea-like organs were observed in the position normally occupied by the palea (Fig. 1, K and L; Supplemental Fig. S1A). Interestingly, each palea-like organ consisted of two mrps and a smaller bop with two vascular bundles (Fig. 1, L–O). The mrp and bop each had a texture similar to that of the wild-type palea (Fig. 1, M and N). *OsMADS1*, *OsMADS14*, and *OsMADS15* were expressed normally (Fig. 1U), whereas *DL* was not expressed in the palea-like organs, similar to the case for the wild-type palea (Fig. 1U). *OsMADS6* expression was more intense in the *mfs1-1* palea-like organs than in wild-type paleae (Fig. 1U). These findings suggested that the palea-like organs were degenerated paleae, and the increased *OsMADS6* expression in the palea-like organs was probably caused by the relative abundance of mrp tissues.

In 21% of the *mfs1-1* spikelets, the palea was degenerated to various degrees (Supplemental Fig. S1A). Most of the degenerated palea contained the normal mrp and reduced bop (Supplemental Fig. S1, D and E). On a few occasions, the degenerated palea retained only mrp-like structures that contained a nonsilicified upper epidermis without trichomes and protrusions (Fig. 1, F–H). These results suggested that the development of *mfs1-1* bop was severely affected.

Simultaneously, we also investigated the defects of the inner three whorls in the *mfs1-1* mutant. In the florets (41%) with normal paleae, the identities and

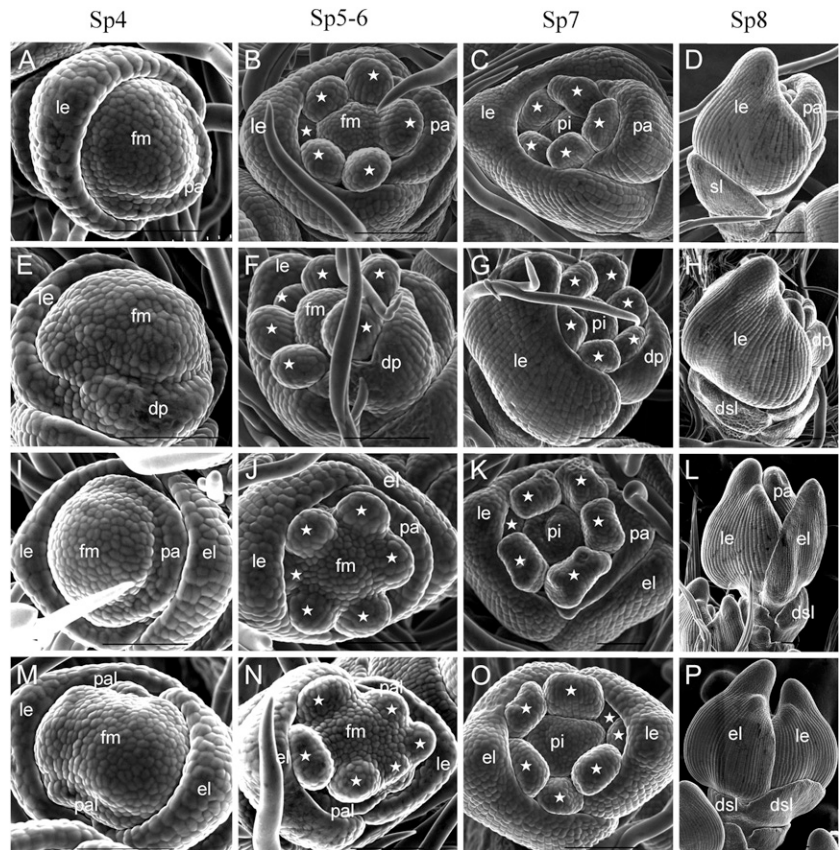
numbers of organs of the inner three whorls were not changed (Supplemental Table S2). In the florets (59%) with degenerated paleae, the numbers of organs of the inner three whorls were varied, but they retained their identities (Supplemental Table S2; Supplemental Fig. S1, F–I). Additionally, 81% of *mfs1-1* spikelets possessed elongated rachillae (Fig. 1, F, I, Q, and S; Supplemental Fig. S1A).

mfs1-1 Exhibited Abnormal Early Spikelet Development

We examined young spikelets of the wild type and mutant at different developmental stages by scanning electron microscopy. During the spikelet 4 stage (Sp4), lemma and palea primordia of the wild-type flower started to develop, and the lemma had a bumped top and was larger than the palea (Fig. 2A). In the *mfs1-1* mutant, some spikelets developed extra lemma-like organ primordia, and their paleae were either normal (Fig. 2I) or degenerated (Fig. 2M). At the same time, the floral meristem was enlarged in parts of the spikelets with degenerated paleae (Fig. 2M). Other spikelets had no extra lemma-like organ, whereas their palea primordia were reduced in size (Fig. 2E). During Sp5 and Sp6, the wild-type flower formed six spherical stamen primordia; the development of one stamen primordium on the lemma side was delayed, whereas the others developed synchronously (Fig. 2B). No significant differences were observed in those florets with an extra lemma-like organ and normal palea (Fig. 2J). However, in some florets with extra lemma-like organs and abnormal paleae, stamen development was not synchronous and the number of stamens varied (Fig. 2, N and O; Supplemental Fig. S1, F and G; Supplemental Table S2). In the florets with degenerated paleae, we found no obvious defects except in terms of the number of stamens (Fig. 2F; Supplemental Table S2). At the Sp7 and Sp8 stages (formation of pistil primordia), the lemma and palea progressed to a further stage of development. In the *mfs1-1* mutant, apparent extra lemma-like organs and degenerated paleae were observed (Fig. 2, H, L, and P).

We also examined the sterile lemma at different developmental stages. At the Sp4 to Sp6 stages, the sterile lemma was larger than the rudimentary glume in the wild type (Fig. 3, A and B). In the *mfs1-1* mutant, the size of the sterile lemma was similar to that of the rudimentary glume (Fig. 3, E and F). At the Sp7 and Sp8 stages, the sterile lemma differentiated drastically and was much larger than the rudimentary glume in the wild type (Fig. 3, C and D). However, the *mfs1-1* sterile lemma was smaller than that of the wild type, resembling the rudimentary glume at these stages (Sp7 and Sp8; Fig. 3, G and H). Meanwhile, the epidermal cells started to elongate in sterile lemmas and still maintained their size in the rudimentary glume in the wild type (Fig. 3D), whereas their sizes were maintained in both the rudimentary glume and the sterile lemma of the *mfs1-1* mutant (Fig. 3H). These results suggested that the identity of

Figure 2. Spikelets at early developmental stages in the wild type and *mfs1-1*. A to D, Wild-type spikelet at stages Sp4 (A), Sp5 to Sp6 (B), Sp7 (C), and Sp8 (D). E to P, *mfs1-1* spikelet at stages Sp4 (E, I, and M), Sp5 to Sp6 (F, J, and N), Sp7 (G, K, and O), and Sp8 (H, L, and P). dsl, Degenerated sterile lemma; el, extra lemma-like organ; fm, floral meristem; le, lemma; lo, lodicule; pa, palea; pal, palea-like organ; pi, pistil; sl, sterile lemma. Asterisks indicate the stamens. Bars = 100 μ m.



the *mfs1-1* sterile lemma was affected, and the sterile lemma in the *mfs1-1* mutant displayed a development pattern similar to that of the rudimentary glume.

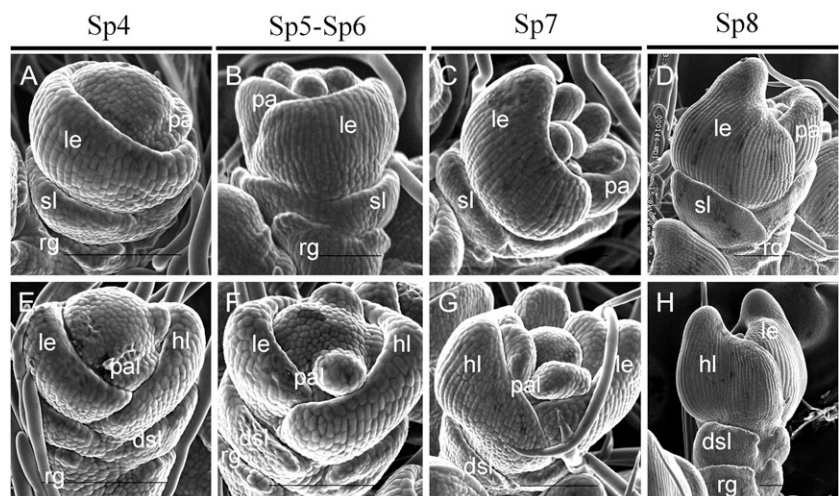
Expression Patterns of Floral Organ Identity Genes during Early Stages of Flower Development

The expression patterns of *DL*, *OsMADS1*, and *OsMADS6*, which are known to be involved in the

regulation of the lemma and palea identities, were investigated during the early stages of flower development.

In wild-type flowers, *DL* was first expressed in the lemma primordia at stages Sp4 to Sp6 (Fig. 4, A and B) and then also in pistil primordia after SP7 (Fig. 4C), whereas *DL* transcripts were still retained in the lemma at Sp8 (Fig. 4D). In *mfs1-1* flowers, the *DL* signals were pronounced in the extra lemma-like organ,

Figure 3. Sterile lemma development in wild-type and *mfs1-1* spikelets at early stages. A to D, Development of the sterile lemma in the wild type at stages Sp4 (A), Sp5 to Sp6 (B), Sp7 (C), and Sp8 (D). E to H, Sterile lemma development in *mfs1-1* at stages Sp4 (E), Sp5 to Sp6 (F), Sp7 (G), and Sp8 (H). dsl, Degenerated sterile lemma; hl, hull-like organ; le, lemma; pa, palea; pal, palea-like organ; rg, rudimentary glume; sl, sterile lemma. Bars = 100 μ m.



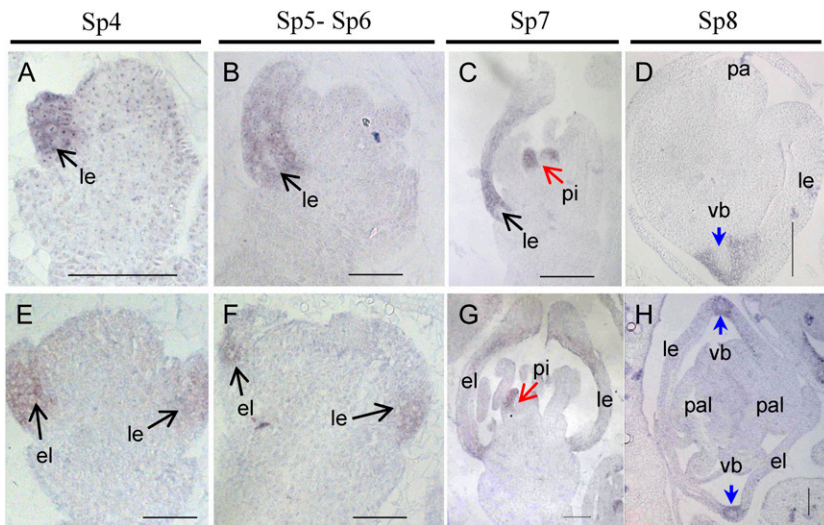


Figure 4. Expression of the *DL* gene in wild-type and *mfs1-1* flowers. A to D, Wild-type flowers. E to H, *mfs1-1* flowers. Columns 1 to 3 show longitudinal sections of flowers at stages Sp4 to Sp7, and column 4 shows transverse sections of flowers at stage Sp8. el, Extra lemma-like organ; le, lemma; pa, palea; pal, palea-like organ; pi, pistil; vb, vascular bundle. Bars = 50 μ m.

in addition to the lemma and pistil (Fig. 4, E–H). These findings proved that the spikelets did indeed develop extra lemmas at the early stage of flower development.

In stages Sp4 to Sp8, *OsMADS1* was expressed in the lemmas and paleae of wild-type florets (Fig. 5, A–D). In the *mfs1-1* mutant, *OsMADS1* signals were observed

in the extra lemma-like organ, lemma, and palea (Fig. 5, E–H). In stages Sp4 to Sp7, *OsMADS6* expression exhibited no significant differences between *mfs1-1* and wild-type flowers and was detected in the floral meristem and primordia of the mrp, lodicule, and pistil (Fig. 5, I–K and M–O). At Sp8, in the transverse

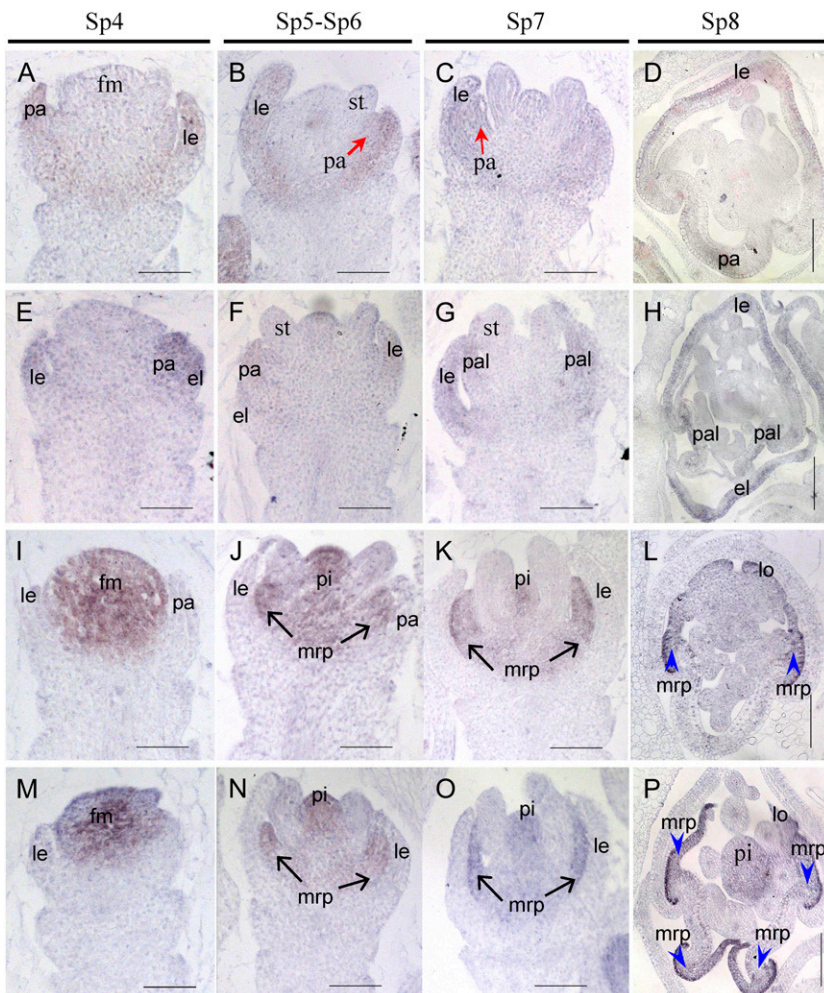


Figure 5. Expression of *OsMADS1* and *OsMADS6* in wild-type and *mfs1-1* flowers. A to D, *OsMADS1* expression in wild-type flowers. E to H, *OsMADS1* expression in *mfs1-1* flowers. I to L *OsMADS6* expression in wild-type flowers. M to P, *OsMADS6* expression in *mfs1-1* flowers. Columns 1 to 3 show longitudinal sections of flowers at stages Sp4 to Sp7, and column 4 shows transverse sections of flowers at stage Sp8. el, Extra lemma-like organ; fm, floral meristem; le, lemma; lo, lodicule; pa, palea; pal, palea-like organ; pi, pistil. Bars = 50 μ m.

section of wild-type florets, *OsMADS6* transcripts were found in the mrp, lodicule, and pistil (Fig. 5L). In the *mfs1-1* mutant, *OsMADS6* signals were detected in the two mrps of each palea-like organ, lodicule, and pistil (Fig. 5P). These results further suggested that the palea-like organs were derived from paleae in the *mfs1-1* mutant.

Molecular Cloning and Identification of *MFS1*

The *MFS1* gene was previously mapped to a region of about 350 kb on chromosome 5 (Ren et al., 2012). Here, the location of *MFS1* was narrowed to within a physical distance of 67 kb between the insertion/deletion markers IND17 and IND24 (Fig. 6A), in which there are 16 annotated genes (<http://www.gramene.org/>). Sequencing analysis identified a single-nucleotide substitution from C to T within a predicted *AP2/ERF* transcription factor (*LOC_Os05g041760*) in different positions of the two *mfs1* alleles, causing amino acid mutations of Ala-66 to Val-66 in the *mfs1-1* mutant and Thr-51 to Ile-51 in the *mfs1-2* mutant (Fig. 6A). To test whether these mutations were causally linked to the mutant phenotype, the *Os05g041760* wild-type genomic fragment that contained the coding sequence, 2,925 bp of sequence upstream of the start codon, and 938 bp of sequence downstream of the stop codon were transformed into *mfs1-1*. As a result of this, the mutant phenotypes were completely rescued in

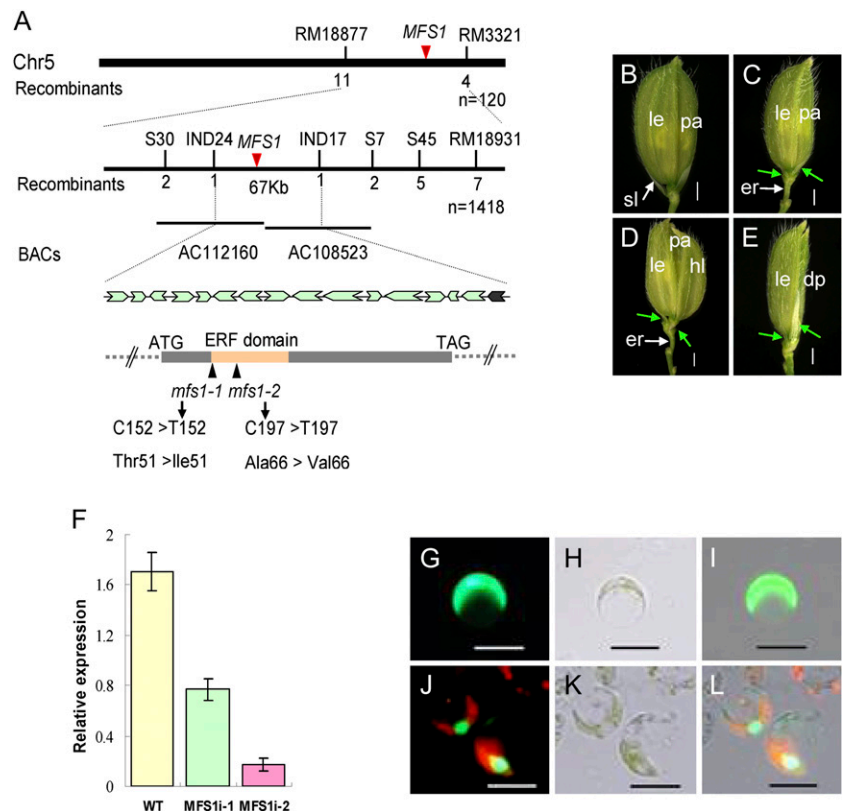
transgenic plants (Supplemental Fig. S2, A–C). We further performed RNA interference (RNAi) to silence *MFS1* in the *japonica* cultivar ZH11. In the transgenic plants, the level of *MFS1* transcript was greatly reduced (Fig. 6F) and pleiotropic spikelet defects similar to those of *mfs1-1* were observed (Fig. 6, B–E). Taken together, these results confirmed that *Os05g041760* is the *MFS1* gene.

***MFS1* Encodes an ERF Domain Protein**

The *AP2/ERF* gene family is plant specific and includes four subfamilies: AP2, RAV, DREB, and ERF (Sharoni et al., 2011). Phylogenetic analysis showed that *MFS1* and its orthologs from moss, gymnosperms, dicots, and grasses constitute an *MFS1*-like clade, whereas the well-known ERF domain proteins FZP and BD1 and their orthologs constitute another clade in the ERF subfamily (Fig. 7). These results suggested that *MFS1*-like and FZP/*BD1*-like genes diverged before the emergence of gymnosperms and that the *MFS1*-like genes differ from the well-known *AP2/ERF* genes. In addition, phylogenetic analysis also showed that the other known *AP2* domain genes (*SNB*, *OsIDS1*, and *SHAT1*) have a distant evolutionary relationship with the *MFS1*-like and FZP/*BD1*-like genes.

Sequence analysis showed that all *MFS1*-like proteins contain a highly conserved ERF domain, located

Figure 6. Isolation of the *MFS1* gene and subcellular localization of the *MFS1* protein. A, Map position of the *MFS1* locus. The relative positions of bacterial artificial chromosome clones (BACs) are shown. Below is the genomic structure of *MFS1*. The sites of the mutation in *mfs1* are shown. Arrows indicate the sites of predicted genes in the IND17 to IND24 interval. B, Phenotype of ZH11 plants. C to F, RNAi analysis of *MFS1* and phenotypes of transgenic plants. C to E, Phenotypes of RNAi transgenic plants. Green arrows indicate the degenerated sterile lemma. dp, Degenerated palea; er, elongated rachilla; hl, hull (lemma/palea)-like organ; le, lemma; pa, palea; sl, sterile lemma. F, *MFS1* expression in RNAi transgenic plants. WT, Wild type. G to L, Analysis of the subcellular localization of the *MFS1* protein using rice protoplasts. G to I, GFP fusion protein. G, Digital image control image. H, Bright-field image. I, Merged image of GFP fusion protein. J to L, *MFS1*-GFP. J, Digital image control image. K, Bright-field image. L, Merged image of *MFS1*-GFP fusion protein. Bars = 1,000 μ m in B to E and 50 μ m in G to L.



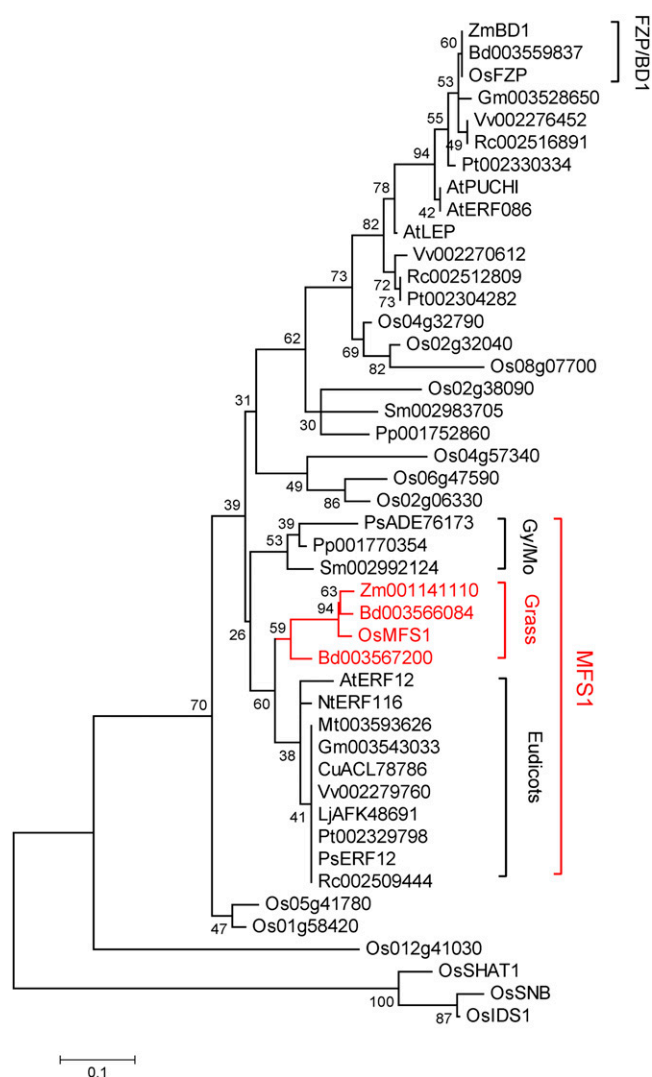


Figure 7. Phylogenetic tree of the MFS1 proteins. The phylogenetic tree was constructed using the maximum likelihood method based on the Jones-Taylor-Thornton matrix-based model. Gy/Mo, Gymnosperms and mosses. [See online article for color version of this figure.]

close to their N terminus. Meanwhile, a conserved C-terminal domain was identified in MFS1-like proteins from grasses and dicots, which share the DLNEPP¹⁸⁵⁻¹⁹⁰ motif. A unique site (V³⁷) and a motif (SPWH¹³²⁻¹³⁵) were also identified in MFS1-like proteins from grasses (Supplemental Fig. S3). In addition, the MFS1 gene shared low sequence similarity with the known AP2/ERF genes outside the AP2/ERF domain (Supplemental Fig. S3).

Vectors that contained the MFS1ORF-GFP fusion protein, the SL1ORF-GFP fusion protein, and the single GFP protein were transiently expressed in rice protoplasts. The SL1ORF-GFP protein acted as a positive nuclear gene control (Xiao et al., 2009). Green fluorescence was detected in the nuclei of rice protoplasts for both MFS1ORF-GFP and SL1ORF-GFP fusion proteins (Fig. 6, J-L; Supplemental Fig. S2, D-F). In cells that

expressed GFP alone, green fluorescence was observed uniformly throughout the cell, apart from the vacuole (Fig. 6, G-I). These results suggest that MFS1 encodes a nuclear protein that may act as a transcription factor.

Expression Patterns of MFS1

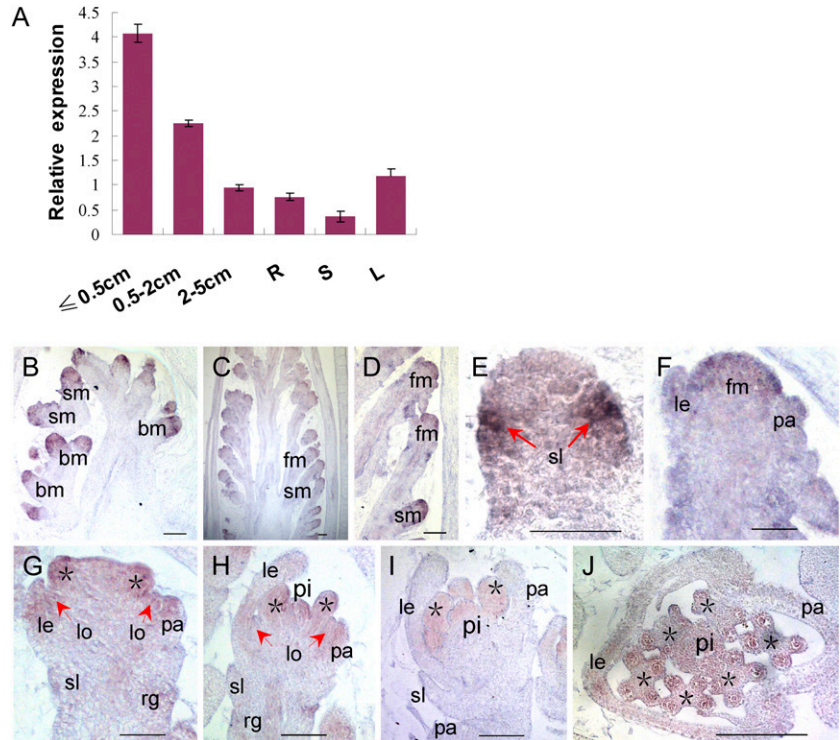
Quantitative reverse transcription-PCR (qPCR) analysis showed that MFS1 was universally expressed in various tissues, including roots, stems, leaves, and panicles, with higher levels in young panicles (2 cm or less) than in the other tissues examined (Fig. 8A). Furthermore, the MFS1 expression pattern was investigated by in situ hybridization. First, MFS1 was highly expressed in the meristems of branches and spikelets (Fig. 8, B-D). Next, strong signals were observed at the sites of initiation of the sterile lemma primordium (Fig. 8E). When the lemma and palea primordia formed, abundant MFS1 transcripts were detected in the lemma, palea, and floral meristem (Fig. 8, D, F, and G). Subsequently, the expression of MFS1 was primarily restricted to the lemma, palea, lodicule, and stamen (Fig. 8, G and H). After the formation of pistil, MFS1 signals disappeared from the lemma and palea but were retained in the lodicule, stamen, and pistil (Fig. 8, I and J).

MFS1 Affects the Expression of Genes Related to Spikelet Development

Given that the *mfs1-1* mutant exhibited spikelet defects, we examined the expression levels of the *IDS1*-like genes *SNB* and *OsIDS1*, which are closely associated with the transition and determinacy of spikelet meristem in rice (Lee et al., 2007; Lee and An, 2012). *SNB* transcripts accumulated primarily in young panicles less than 2 cm long, and their levels were lower in the *mfs1-1* mutant than in the wild type (Fig. 9A). Then, levels of *SNB* transcripts were dramatically decreased in panicles longer than 2 cm, and no difference in the levels of *SNB* expression was found between wild-type and *mfs1-1* panicles with a length 2 to 5 cm (Fig. 9A). *OsIDS1* transcripts were first detected in young panicles less than 0.5 cm, and they were more abundant in wild-type panicles between 0.5 and 5 cm in length (Fig. 9A). Compared with that in the wild type, *OsIDS1* expression showed no obvious change in panicles with a length less than 0.5 cm, whereas it dramatically decreased in *mfs1-1* panicles 0.5 to 5 cm long (Fig. 9A). These results imply that MFS1 positively regulated the expression of the *IDS1*-like genes *SNB* and *OsIDS1*.

We used qPCR to examine the expression of the *G1* gene, which has been shown to be involved in the specification of sterile lemma identity (Yoshida et al., 2009; Hong et al., 2010). In the wild type, a high level of *G1* expression was detected in panicles shorter than 2 cm, but the mRNA levels were significantly reduced in those that were 2 to 5 cm (Fig. 9A). In the *mfs1-1* mutant, *G1* showed lower expression levels in young panicles shorter than 5 cm (Fig. 9A). In situ

Figure 8. Expression pattern of *MFS1*. A, *MFS1* expression in different tissues as detected by qPCR. R, Root; S, stem; L, leaf. B to J, In situ hybridization in wild-type panicles and flowers using an *MFS1* antisense probe. bm, Branch meristem; fm, floral meristem; le, lemma; lo, lodicule; pa, palea; pi, pistil; rg, rudimentary glume; sl, sterile lemma; sm, spikelet meristem. Asterisks indicate the stamens. Bars = 50 μ m.



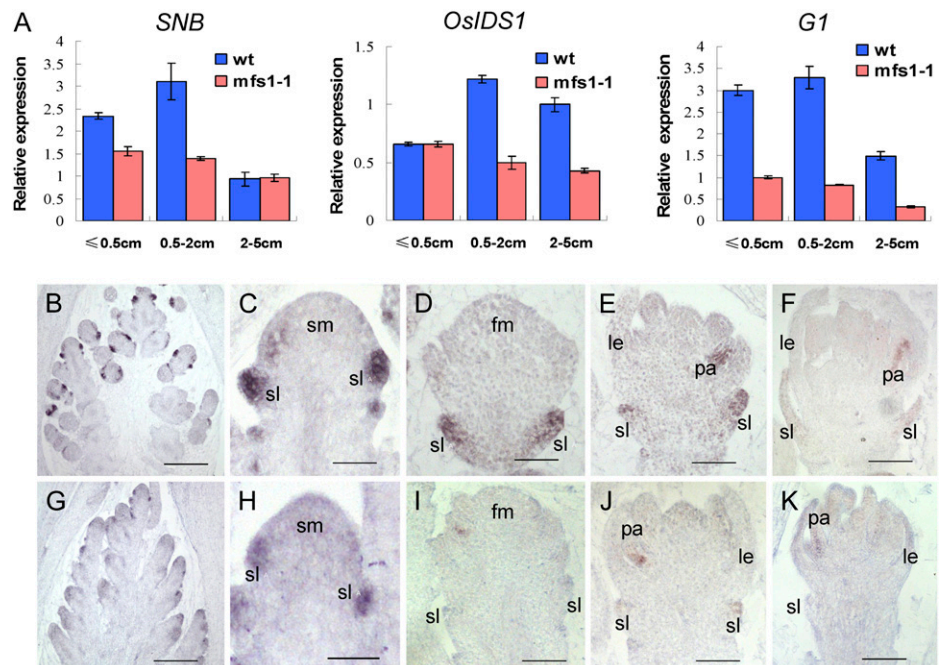
hybridization indicated that in the wild type, the *G1* signals were strongly detected in sterile lemmas during the stage of sterile lemma primordia differentiation and formation, and subsequently, they decreased markedly when sterile lemmas started to elongate (Fig. 9, B–F). *G1* expression was faint in the sterile lemma primordia of the *mfs1-1* spikelet during the stages analyzed (Fig. 9, G–K), consistent with the results of

qPCR analysis. These findings suggest that *MFS1* positively regulates *G1* expression.

DISCUSSION

In this study, we characterized a novel *AP2/ERF* domain gene, *MFS1*, that is involved in the regulation of spikelet meristem determinacy and floral organ

Figure 9. Expression of *SNB*, *OsIDS1*, and *G1* in wild-type and *mfs1-1* flowers. A, qPCR analysis of *SNB*, *OsIDS1*, and *G1* in developing wild-type (wt) and *mfs1-1* panicles at different stages. B to F, *G1* expression in wild-type flowers. G to K, *G1* expression in *mfs1-1* flowers. le, Lemma; lo, lodicule; pa, palea; sl, sterile lemma; sm, spikelet meristem. Bars = 50 μ m.



identity in rice. *MFS1* promotes the expression of the *SNB*, *OsIDS1*, and *G1* genes involved in the development of spikelets.

MFS1 Affects Spikelet Meristem Determinacy

Most spikelets in *mfs1-1* mutant plants each developed an extra lemma. About 27% of these spikelets produced normal florets after the extra lemmas arose, which suggested that these spikelets were composed of a terminal floret and a degenerated lateral floret that only contained the lemma. In the other spikelets with abnormal florets, two palea-like organs were observed, which corresponded to the extra lemma and the original lemma. Together with the development of a floral meristem that reached a larger than usual size at an earlier stage (Fig. 2M), these results imply that these spikelets tended to produce two florets, and the spikelet meristem determinacy was disturbed in the *mfs1-1* mutant. Similarly, in the *tongari-boushi1* (*tob1*) mutant, some spikelets had an extra lemma/palea-like organ between the sterile lemma and the original lemma (Tanaka et al., 2012). In the *snb* mutant, some spikelets developed supernumerary rudimentary glumes, extra lemma- or palea-like structures, or lateral florets before the terminal floret emerged (Lee et al., 2007). The *snb+osids1* double mutant even produced more bract-like organs, including rudimentary glumes, lemmas, or paleae, than single mutants (Lee and An, 2012). These results suggest that *SNB*, *OsIDS1*, *TOB1*, and *MFS1* regulate the fate of the spikelet meristem by ensuring the correct timing of the transition of the spikelet meristem to the terminal floral meristem. In contrast, the loss of spikelet meristem determinacy occurred before the formation of the rudimentary glume in *snb* and *osids1* mutants but after the emergence of sterile lemmas in *tob1* and *mfs1-1* mutants. This suggested that *MFS1* and *TOB1* function later than *SNB* and *OsIDS1*. Additionally, decreases in the expression of *SNB* and *OsIDS1* were found in *mfs1-1* mutant young panicles, which suggested that *MFS1* positively regulated the expression of *SNB* and *OsIDS1*.

MFS1 Specifies Sterile Lemma Identity

In the *mfs1-1* mutant, the degenerated sterile lemma exhibited the identities of both the sterile lemma and the rudimentary glume. In the *snb* mutant, no sterile lemmas were found at sites where extra rudimentary glumes were present (Lee et al., 2007), which suggested the homeotic transformation of the sterile lemma to the rudimentary glume. In the *osids1* mutant, one of the sterile lemmas was shown to be occasionally replaced by a rudimentary glume (Lee and An, 2012). *SNB* and *OsIDS1* were also previously shown to encode an AP2/ERF domain protein (Lee et al., 2007; Lee and An, 2012). These results suggest that *MFS1*, *SNB*, and *OsIDS1* confer important functions in the development of

the sterile lemma. It was reported that *G1/ELE*, *OsMADS34*, and *EG1* determined the identity of the sterile lemma. In these mutants, the sterile lemma was homeotically transformed into the lemma (Li et al., 2009; Yoshida et al., 2009; Gao et al., 2010; Hong et al., 2010; Kobayashi et al., 2010). These results suggest that *G1/ELE*, *OsMADS34*, and *EG1* prevent the transformation of the sterile lemma to the lemma, whereas *MFS1*, *SNB*, and *OsIDS1* prevent the degeneration of the sterile lemma to the rudimentary glume.

There have been two prevailing hypotheses on the origin and evolution of the sterile lemma (Takeoka et al., 1993). One states that a putative ancestor of the genus *Oryza* had a spikelet that contained a terminal floret and two lateral florets, which subsequently degenerated during evolution, leaving only the lemma (Arber, 1934; Kellogg, 2009). The sterile lemma thus would seem to be derived from morphological modification of the remnants of this lemma (Yoshida et al., 2009; Kobayashi et al., 2010). The other hypothesis suggests that the spikelet of *Oryza* spp. has only one floret, and the sterile lemma and rudimentary glume are universally regarded as severely reduced bract structures (Schmidt and Ambrose, 1998; Terrell et al., 2001; Hong et al., 2010). In the *g1/ele1*, *osmads34*, and *eg1* mutants, the sterile lemmas were enlarged and transformed into lemmas, which supports the first hypothesis. In the *mfs1-1* mutant, the sterile lemma was degenerated and acquired the identity of the rudimentary glume, which supports the second hypothesis. In fact, in most grass species, the spikelet lacks sterile lemma-like organs and only contains one or more florets and bract-like glume organs, which are considered to be equivalent to the rudimentary glumes of *Oryza* spp. (Takeoka et al., 1993; Yoshida et al., 2009; Hong et al., 2010). The bract-like glume organ resembles the lemma in size and structure in some grass species, such as maize and wheat (Kellogg, 2001; Yoshida et al., 2009), whereas it is severely reduced in *Oryza* spp. (Bommert et al., 2005; Li et al., 2009). Therefore, the lemma, sterile lemma, and rudimentary glume may be homologous structures.

MFS1 Regulates Palea Development

In grass flowers, the palea was thought to have a different identity and origin from the lemma. In general, the palea is considered homologous to the prophyll (the first leaf produced by the axillary meristem) that is formed on a floret axis, whereas the lemma corresponds to the bract (the leaf subtending the axillary meristem) that is formed on a spikelet axis (Kellogg, 2001; Ohmori et al., 2009). Recently, some evidence has indicated that the rice palea is an organ produced by congenital fusion of the *bop* and the *mrp*, which potentially have distinct origins (Francis, 1920; Cusick, 1966; Verbeke, 1992; Zanis, 2007). Specifically, first, the cellular structure of the *bop* was shown to be highly similar to that of the lemma but distinct from that of the *mrp* (Prasad et al., 2005; Sang et al., 2012).

Second, the rice B-class mutant *superwoman1* (*spw1/osmads16*) and *MADS2+MADS4* double RNAi plants showed transformation of the lodicules into organs that resembled the mrp but not the bop. Moreover, mutants of Arabidopsis B-class genes undergo homeotic transformation of petals (equivalent to lodicules) into sepals (Nagasawa et al., 2003; Yadav et al., 2007; Yao et al., 2008). These findings suggest that the mrp, but not bop, is homologous to the sepal. In the *depressed palea1* (*dp1*) mutant, the palea was shown to be replaced by two mrp-like structures and the bop was lost (Luo et al., 2005; Jin et al., 2011). In the *retarded palea1* (*rep1*) mutant, the development of the bop was delayed, whereas overexpression of *REP1* caused overdifferentiation of the mrp cells (Yuan et al., 2009). In the *mfs1-1* mutant, the bop was degenerated in most florets and was even absent in a few cases. Additionally, recent studies revealed that *CHIMERIC FLORAL ORGANS1* (*CFO1/OsMADS32*) and *MOSAIC FLORAL ORGANS1* (*MFO1/OsMADS6*) were expressed in the mrp, the mutations of which resulted in transformation of the mrp into lemma-like or bop structures (Ohmori et al., 2009; Li et al., 2010; Sang et al., 2012). These results indicated that two parts of the palea are controlled by different regulatory pathways. Whereas *MFS1*, *DP1*, and *REP1* determine bop identity, *MFO1* and *CFO1* are involved in the regulation of mrp identity. Consistent with these hypotheses, the phenotypes of the *mfs1* palea suggest that the rice palea is an organ produced by the fusion of the mrp and bop, which have different origins.

CONCLUSION

In this study, we characterized the rice *MFS1* gene, which belongs to a clade of unknown function in the *AP2/ERF* gene family. The *mfs1* spikelets displayed extra lemmas, degenerated sterile lemmas, and paleae. These results suggest that *MFS1* plays an important role in the regulation of spikelet determinacy and organ identity. Our data also reveal that *MFS1* positively regulates the expression of *G1* and the *IDS1*-like genes *SNB* and *OsIDS1*.

MATERIALS AND METHODS

Plant Materials

Two mutants of rice (*Oryza sativa*), *mfs1-1* and *mfs1-2*, were identified from ethylmethane sulfonate-treated cultivar Jinhui 10. cv Jinhui 10 was used as the wild-type strain for phenotypic observation. All plants were cultivated in paddies in Chongqing and Hainan, China.

Map-Based Cloning of *MFS1*

The *mfs1-1* mutant was crossed with cv Xinong1A, and 1,418 F2 plants with the mutational phenotype were selected and used as a mapping population. Initial gene mapping was conducted using simple sequence repeat markers from publicly available rice databases, including Gramene (<http://www.gramene.org>) and the Rice Genomic Research Program (<http://rgp.dna.affrc.go.jp/publicdata/caps/index.html>). Then, fine-mapping was performed using

insertion/deletion markers developed from comparisons of genomic sequences from cv Xinong1A and Jinhui 10 in our laboratory. The sequences of primers used in the mapping and candidate gene analysis are listed in Supplemental Table S1.

Microscopy Analysis

Panicles were collected at different developmental stages and fixed in 50% ethanol, 0.9 M glacial acetic acid, and 3.7% formaldehyde overnight at 4°C, dehydrated with a graded ethanol series, infiltrated with xylene, and embedded in paraffin (Sigma). The 8- μ m-thick sections were transferred onto poly-L-Lys-coated glass slides, deparaffinized in xylene, and dehydrated through an ethanol series. The sections were stained sequentially with 1% safranin (Amresco) and 1% Fast Green (Amresco), then dehydrated through an ethanol series, infiltrated with xylene, and finally mounted beneath a coverslip. Light microscopy was performed using a Nikon E600 microscope. For scanning electron microscopy, fresh samples were examined using a Hitachi S-3400 scanning electron microscope with a -20°C cool stage. The stages of early spikelet development were the same as those defined previously (Ikeda et al., 2004).

RNA Isolation and qPCR Analysis

RNA from root, stem, leaf, inflorescence, and young flower was isolated using the RNeasy Plant Mini Kit from Watson. The first strand of complementary DNA was synthesized from 2 μ g of total RNA using oligo(dT)₁₈ primers in a 25- μ L reaction volume using the SuperScript III Reverse Transcriptase Kit (Invitrogen). Reverse-transcribed RNA (0.5 μ L) was used as a PCR template with gene-specific primers (Supplemental Table S3). The qPCR analysis was performed with an ABI Prism 7000 Sequence Detection System and the SYBR Supermix Kit (Bio-Rad). At least three replicates were performed, and mean values for the expression of each gene were used.

In Situ Hybridization

The 482-bp gene-specific *MFS1* probe was amplified with the primers *MFS1-F* and *MFS1-R* and labeled using the DIG RNA Labeling Kit (SP6/T7) from Roche. Probes for the known floral organ genes were prepared using the same method. Pretreatment of sections, hybridization, and immunological detection were performed as described previously (Sang et al., 2012). The primer sequences are listed in Supplemental Table S1.

Vector Construction

For the complementation test, a 4,433-bp genomic fragment that contained the *MFS1* coding sequence, coupled with the 2,925-bp upstream and 938-bp downstream sequences, was amplified using the primers *MFS1com-F* and *MFS1com-R*. The resulting PCR products were digested using *Xba*I and *Eco*RI and then inserted into the binary vector pCAMBIA1301. The recombinant plasmids were introduced into *mfs1-1* by the *Agrobacterium tumefaciens*-mediated transformation method as described previously (Sang et al., 2012). To make a construct for RNAi, we amplified a 267-bp fragment of *MFS1* complementary DNA with the primers *MFS1Ri-F* (*Spe*I, *Kpn*I) and *MFS1Ri-R* (*Sac*I, *Bam*HI), as shown in Supplemental Table S1. The resulting PCR products were first digested using *Spe*I and *Sac*I and then ligated into vector pTCK303 (Wang et al., 2004) to obtain the intermediate vector. The PCR products were then digested using *Kpn*I and *Bam*HI and ligated into the intermediate vector. The recombinant plasmids were transformed into ZH11 plants by the *A. tumefaciens*-mediated transformation method. The primer sequences are listed in Supplemental Table S1.

Subcellular Localization

The coding region of *MFS1* without the stop codon was amplified using the primer pair *MFS1OE-F* and *MFS1OE-R* which contain *Xba*I and *Bam*HI sites, respectively (Supplemental Table S1). The fragment was cloned into the expression cassette 35S-GFP (S65T)-NOS (pCAMBIA1301) with appropriate modifications, which generated the *MFS1-GFP* fusion vector. The GFP and *MFS1-GFP* plasmids were transformed into rice protoplasts as described previously (Li et al., 2009). After 8 to 16 h of incubation at 28°C, GFP fluorescence was observed with a Nikon E600 microscope.

Protein Sequence and Phylogenetic Analysis

Protein sequences were obtained by searching GenBank (<http://www.ncbi.nlm.nih.gov/genbank/>) using the MFS1 sequence as a query. A phylogenetic tree was constructed using MEGA 5.0 (Tamura et al., 2011). The tree was constructed using the maximum likelihood method based on the JTT matrix-based model with the lowest Bayesian Information Criterion scores (Jones et al., 1992; Tamura et al., 2011). Bootstrap support values for each node from 500 replicates are shown next to the branches (Felsenstein, 1985). The initial tree for the heuristic search was obtained automatically as follows. When the number of common sites was less than 100 or less than one-quarter of the total number of sites, the maximum parsimony method was used; otherwise, the bio-neighbor-joining method with Markov Cluster distance matrix was used. A discrete γ -distribution was used to model evolutionary rate differences among sites (five categories [+G], parameter = 0.6362). The tree was drawn to scale, with branch lengths measured in terms of the number of substitutions per site.

Sequence data from this article can be found in the GenBank/EMBL data libraries under accession numbers: *SNB* (ABD24033), *OsIDS1* (NM_001058244), *G1/ELE* (AB512480), *DL* (AB106553), *OsMADS1* (NM_001055911), *OsMADS6* (FJ666318), *OsMADS14* (NM_001057835), and *OsMADS15* (NM_001065255).

Supplemental Data

The following materials are available in the online version of this article.

Supplemental Figure S1. Investigation of *mfs1* spikelets.

Supplemental Figure S2. Complementation test and subcellular localization.

Supplemental Figure S3. Protein sequence alignment of the closely related *AP2/ERF* genes.

Supplemental Table S1. Primers used in the study.

Supplemental Table S2. Distribution of the number of floral organs in the wild type and *mfs1-1*.

Received January 17, 2013; accepted April 26, 2013; published April 29, 2013.

LITERATURE CITED

- Ambrose BA, Lerner DR, Ciceri P, Padilla CM, Yanofsky MF, Schmidt RJ (2000) Molecular and genetic analyses of the *silky1* gene reveal conservation in floral organ specification between eudicots and monocots. *Mol Cell* 5: 569–579
- Arber A (1934) *The Gramineae: A Study of Cereal, Bamboo, and Grasses*. Cambridge University Press, Cambridge, UK
- Bommert P, Satoh-Nagasawa N, Jackson D, Hirano HY (2005) Genetics and evolution of inflorescence and flower development in grasses. *Plant Cell Physiol* 46: 69–78
- Bradley D, Ratcliffe O, Vincent C, Carpenter R, Coen E (1997) Inflorescence commitment and architecture in Arabidopsis. *Science* 275: 80–83
- Cacharrón J, Saedler H, Theißen G (1999) Expression of MADS box genes *ZMM8* and *ZMM14* during inflorescence development of *Zea mays* discriminates between the upper and the lower floret of each spikelet. *Dev Genes Evol* 209: 411–420
- Clifford HT (1987) Spikelet and floral morphology. In TR Soderstrom, KW Hilu, CS Campbell, ME Barkworth, eds, *Grass Systematics and Evolution*. Smithsonian Institution Press, Washington, DC, pp 21–30
- Chuck G, Meeley RB, Hake S (1998) The control of maize spikelet meristem fate by the *APETELA2*-like gene indeterminate *spikelet1*. *Genes Dev* 12: 1145–1154
- Chuck G, Meeley R, Hake S (2008) Floral meristem initiation and meristem cell fate are regulated by the maize AP2 genes *ids1* and *sid1*. *Development* 135: 3013–3019
- Coen ES, Meyerowitz EM (1991) The war of the whorls: genetic interactions controlling flower development. *Nature* 353: 31–37
- Coen ES, Nugent JM (1994) Evolution of flowers and inflorescences. *Development (Suppl)* 107–116
- Cusick F (1966) On phylogenetic and ontogenetic fusions. In EG Cutter, ed, *Trends in Plant Morphogenesis*. Longmans, Green, London, pp 170–183
- Dreni L, Jacchia S, Fornara F, Fornari M, Ouwerkerk PB, An G, Colombo L, Kater MM (2007) The D-lineage MADS-box gene *OsMADS13* controls ovule identity in rice. *Plant J* 52: 690–699
- Felsenstein J (1985) Confidence limits on phylogenies: an approach using the bootstrap. *Evolution* 39: 783–791
- Francis ME (1920) *Book of Grasses*. Doubleday, Page, Garden City, NY
- Gao XC, Liang WQ, Yin CS, Ji SM, Wang HM, Su X, Guo C, Kong HZ, Xue HW, Zhang DB (2010) The SEPALLATA-like gene *OsMADS34* is required for rice inflorescence and spikelet development. *Plant Physiol* 153: 728–740
- Hong L, Qian Q, Zhu K, Tang D, Huang Z, Gao L, Li M, Gu M, Cheng Z (2010) ELE restrains empty glumes from developing into lemmas. *J Genet Genomics* 37: 101–115
- Ikeda K, Sunohara H, Nagato Y (2004) Developmental course of inflorescence and spikelet in rice. *Breed Sci* 54: 147–156
- Itoh J, Nonomura K, Ikeda K, Yamaki S, Inukai Y, Yamagishi H, Kitano H, Nagato Y (2005) Rice plant development: from zygote to spikelet. *Plant Cell Physiol* 46: 23–47
- Jeon JS, Jang S, Lee S, Nam J, Kim C, Lee SH, Chung YY, Kim SR, Lee YH, Cho YG, et al (2000) *leafy hull sterile1* is a homeotic mutation in a rice MADS box gene affecting rice flower development. *Plant Cell* 12: 871–884
- Jin Y, Luo Q, Tong H, Wang A, Cheng Z, Tang J, Li D, Zhao X, Li X, Wan J, et al (2011) An AT-hook gene is required for palea formation and floral organ number control in rice. *Dev Biol* 359: 277–288
- Jones DT, Taylor WR, Thornton JM (1992) The rapid generation of mutation data matrices from protein sequences. *Comput Appl Biosci* 8: 275–282
- Kellogg EA (2001) Evolutionary history of the grasses. *Plant Physiol* 125: 1198–1205
- Kellogg EA (2007) Floral displays: genetic control of grass inflorescences. *Curr Opin Plant Biol* 10: 26–31
- Kellogg EA (2009) The evolutionary history of Ehrhartoideae, Oryzaceae, and Oryza. *Rice* 2: 1–14
- Kobayashi K, Maekawa M, Miyao A, Hirochika H, Kyojuka J (2010) *PANICLE PHYTOMER2 (PAP2)*, encoding a SEPALLATA subfamily MADS-box protein, positively controls spikelet meristem identity in rice. *Plant Cell Physiol* 51: 47–57
- Lee DY, An G (2012) Two AP2 family genes, *Supernumerary bract (SNB)* and *Osindeterminate spikelet 1 (OsIDS1)*, synergistically control inflorescence architecture and floral meristem establishment in rice. *Plant J* 69: 445–461
- Lee DY, Lee J, Moon S, Park SY, An G (2007) The rice heterochronic gene *SUPERNUMERARY BRACT* regulates the transition from spikelet meristem to floral meristem. *Plant J* 49: 64–78
- Li H, Liang W, Jia R, Yin C, Zong J, Kong H, Zhang D (2010) The AGL6-like gene *OsMADS6* regulates floral organ and meristem identities in rice. *Cell Res* 20: 299–313
- Li M, Xiong G, Li R, Cui J, Tang D, Zhang B, Pauly M, Cheng Z, Zhou Y (2009) Rice cellulose synthase-like D4 is essential for normal cell-wall biosynthesis and plant growth. *Plant J* 60: 1055–1069
- Luo Q, Zhou K, Zhao X, Zeng Q, Xia H, Zhai W, Xu J, Wu X, Yang H, Zhu L (2005) Identification and fine mapping of a mutant gene for palealess spikelet in rice. *Planta* 221: 222–230
- Malcomber ST, Kellogg EA (2004) Heterogeneous expression patterns and separate roles of the SEPALLATA gene *LEAFY HULL STERILE1* in grasses. *Plant Cell* 16: 1692–1706
- Malcomber ST, Preston JC, Reinheimer R, Kossuth J, Kellogg EA (2006) Developmental gene evolution and the origin of grass inflorescence diversity. In J Leebens-Mack, DE Soltis, PS Soltis, eds, *Developmental Genetics of the Flower*. Academic Press, New York, pp 383–421
- Mimida N, Goto K, Kobayashi Y, Araki T, Ahn JH, Weigel D, Murata M, Motoyoshi F, Sakamoto W (2001) Functional divergence of the *TFL1*-like gene family in *Arabidopsis* revealed by characterization of a novel homologue. *Genes Cells* 6: 327–336
- Nagasawa N, Miyoshi M, Sano Y, Satoh H, Hirano H, Sakai H, Nagato Y (2003) *SUPERWOMAN1* and *DROOPING LEAF* genes control floral organ identity in rice. *Development* 130: 705–718
- Nakagawa M, Shimamoto K, Kyojuka J (2002) Overexpression of *RCN1* and *RCN2*, rice *TERMINAL FLOWER 1/CENTRORADIALIS* homologs, confers delay of phase transition and altered panicle morphology in rice. *Plant J* 29: 743–750

- Ohmori S, Kimizu M, Sugita M, Miyao A, Hirochika H, Uchida E, Nagato Y, Yoshida H (2009) *MOSAIC FLORAL ORGANS1*, an *AGL6*-like MADS box gene, regulates floral organ identity and meristem fate in rice. *Plant Cell* **21**: 3008–3025
- Prasad K, Parameswaran S, Vijayraghavan U (2005) OsMADS1, a rice MADS-box factor, controls differentiation of specific cell types in the lemma and palea and is an early-acting regulator of inner floral organs. *Plant J* **43**: 915–928
- Rao NN, Prasad K, Kumar PR, Vijayraghavan U (2008) Distinct regulatory role for RFL, the rice LFY homolog, in determining flowering time and plant architecture. *Proc Natl Acad Sci USA* **105**: 3646–3651
- Ratcliffe OJ, Bradley DJ, Coen ES (1999) Separation of shoot and floral identity in *Arabidopsis*. *Development* **126**: 1109–1120
- Ren DY, Li YF, Wang Z, Xu FF, Guo S, Zhao FM, Sang XC, Ling YH, He GH (2012) Identification and gene mapping of a multi-floret spikelet 1 (*mfs1*) mutant associated with spikelet development in rice. *J Integr Agric* **11**: 1574–1579
- Sang XC, Li YF, Luo ZK, Ren DY, Fang LK, Wang N, Zhao FM, Ling YH, Yang ZL, Liu YS, et al (2012) *CHIMERIC FLORAL ORGANS1*, encoding a monocot-specific MADS box protein, regulates floral organ identity in rice. *Plant Physiol* **160**: 788–807
- Schmidt RJ, Ambrose BA (1998) The blooming of grass flower development. *Curr Opin Plant Biol* **1**: 60–67
- Sharoni AM, Nuruzzaman M, Satoh K, Shimizu T, Kondoh H, Sasaya T, Choi IR, Omura T, Kikuchi S (2011) Gene structures, classification and expression models of the AP2/EREBP transcription factor family in rice. *Plant Cell Physiol* **52**: 344–360
- Sussex IM, Kerk NM (2001) The evolution of plant architecture. *Curr Opin Plant Biol* **4**: 33–37
- Takeoka Y, Shimizu M, Wada T (1993) Panicles. In T Matsuo, K Hoshikawa, eds, *Science of the Rice Plant*, Vol I. Nobunkyo, Tokyo, pp 295–326
- Tamura K, Peterson D, Peterson N, Stecher G, Nei M, Kumar S (2011) MEGA5: molecular evolutionary genetics analysis using maximum likelihood, evolutionary distance, and maximum parsimony methods. *Mol Biol Evol* **28**: 2731–2739
- Tanaka W, Toriba T, Ohmori Y, Yoshida A, Kawai A, Mayama-Tsuchida T, Ichikawa H, Mitsuda N, Ohme-Takagi M, Hirano H (2012) The *YABBY* gene *TONGARI-BOUSHII1* is involved in lateral organ development and maintenance of meristem organization in the rice spikelet. *Plant Cell* **24**: 80–95
- Terrell EE, Peterson PM, Wergin WP (2001) Epidermal features and spikelet micromorphology in *Oryza* and related genera (Poaceae: Oryzoideae). *Smithsonian Contr Bot* **91**: 1–50
- Verbeke JA (1992) Fusion events during floral morphogenesis. *Annu Rev Plant Physiol Plant Mol Biol* **43**: 583–598
- Wang M, Chen C, Xu YY, Jiang RX, Han Y, Xu ZH, Chong K (2004) A practical vector for efficient knockdown of gene expression in rice (*Oryza sativa* L.). *Plant Mol Biol Rep* **22**: 409–417
- Weberling F (1989) *Morphology of Flowers and Inflorescence*. Cambridge University Press, Cambridge, UK
- Xiao H, Tang J, Li Y, Wang W, Li X, Jin L, Xie R, Luo H, Zhao X, Meng Z, et al (2009) *STAMENLESS 1*, encoding a single C2H2 zinc finger protein, regulates floral organ identity in rice. *Plant J* **59**: 789–801
- Yadav SR, Prasad K, Vijayraghavan U (2007) Divergent regulatory OsMADS2 functions control size, shape and differentiation of the highly derived rice floret second-whorl organ. *Genetics* **176**: 283–294
- Yao SG, Ohmori S, Kimizu M, Yoshida H (2008) Unequal genetic redundancy of rice *PISTILLATA* orthologs, OsMADS2 and OsMADS4, in lodicule and stamen development. *Plant Cell Physiol* **49**: 853–857
- Yoshida A, Suzaki T, Tanaka W, Hirano HY (2009) The homeotic gene long sterile lemma (*G1*) specifies sterile lemma identity in the rice spikelet. *Proc Natl Acad Sci USA* **106**: 20103–20108
- Yuan Z, Gao S, Xue DW, Luo D, Li LT, Ding SY, Yao X, Wilson ZA, Qian Q, Zhang DB (2009) *RETARDED PALEA1* controls palea development and floral zygomorphy in rice. *Plant Physiol* **149**: 235–244
- Zahn LM, Kong H, Leebens-Mack JH, Kim S, Soltis PS, Landherr LL, Soltis DE, Depamphilis CW, Ma H (2005) The evolution of the *SEPALLATA* subfamily of MADS-box genes: a preangiosperm origin with multiple duplications throughout angiosperm history. *Genetics* **169**: 2209–2223
- Zanis MJ (2007) Grass spikelet genetics and duplicate gene comparisons. *Int J Plant Sci* **168**: 93–110